ELEVATION BEAM PROFILE CONTROL WITH BIAS POLARITY PATTERNS APPLIED TO MICROFABRICATED ULTRASOUND TRANSDUCERS

Chris Daft, Paul Wagner, Satchi Panda and Igal Ladabaum
Sensant Corp., 14470 Doolittle Drive, San Leandro, CA 94577, USA

Abstract — In contrast to PZT probes, Capacitive Microfabricated Ultrasonic Transducers (cMUTs) require a DC bias. We investigate elevation beam profile shaping by spatially varying this bias polarity. Such a scheme introduces a 180° phase shift in the device's impulse response. A Fresnel zone plate is realized which is capable of generating tight elevation foci using a large aperture. This paper presents measurements from a prototype Fresnel cMUT probe, and matching simulation results. The Fresnel probe is capable of improved slice thickness compared with both a conventionally lensed probe and a multi-row design. Also, combinations of bias polarity control and multiple firings can enable harmonic imaging without pre-distortion of the transmit signal. Multiple firing schemes further optimize slice thickness, and allow beam steering in elevation.

I. INTRODUCTION

cMUTs [1] have attracted attention due to their broadband performance, and potential for use with integrated electronics and 3-D imaging. The clinical value of thinner and more uniform slices is well established, and much work has been done (e.g. [2]) to improve upon the traditional silicone lens which works well only at one range. Elsewhere, it creates volume averaging artifacts that obscure important image features. Moreover, slice thickness advances achieved by the GE *Active Matrix Arrays* [3] and Siemens *Multi-D* transducers frequently improve diagnostic productivity. The sonographer can avoid trying several approaches before a view insensitive to slice thickness is found. cMUTs can provide slice thickness control through varying the polarity of the bias voltage in elevation. Performance compares favorably with existing multi-row technologies and offers significantly lower interconnect complexity. An extension of this idea permits accurate harmonic imaging at high output powers.

II. VARYING BIAS VOLTAGE IN ELEVATION

The Mason equivalent circuit for a cMUT includes a transformer [4] which converts between electrical current and mechanical force. This has a turns ratio n proportional to the DC bias voltage:

$$n \approx C\, V_{\text{bias}} / d$$

where C is the device capacitance and d is the electrode spacing. A patterned metallization defines the azimuth elements on one side of the device; traditionally the other side has been a continuous electrode. This continuous electrode can be replaced with bias lines orthogonal to the azimuth elements. This allows a given azimuth element to have a bias voltage that varies in elevation without disturbing the imager's azimuth focusing. A pattern of bias voltages can be used as a Fresnel lens [5] to focus in elevation. Multiple focal zones are typically used in radiology so that the focus can be adjusted for each zone. Figure 1 shows how the elevation bias pattern can also be optimized on a per-zone basis.

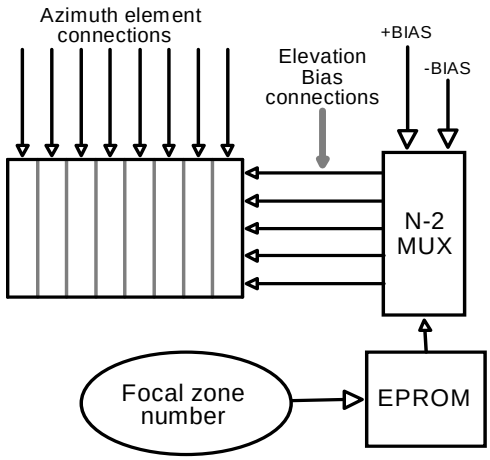

Figure 1: Bias control in elevation. The aperture can be driven by a simple representation of the focal zone number from the imager.

III. SIMULATION AND EXPERIMENT

As well as focusing at a specified depth, we can turn off parts of the aperture by alternating the bias pattern at high spatial frequency. To test both apodizing and focusing, we constructed a transducer with a 10 MHz center frequency, 192 elements and 1.4 λ pitch. 0.6 λ-spaced bias connections were created in a 10 mm elevation aperture. An elevation of 67 λ is several times larger than would be expected in a standard linear array. The active elevation control increases the allowable aperture, with concomitant penetration improvement. The on-axis impulse response was measured with all of its bias lines connected to +120 V, then with all lines connected to −120 V, and then with interleaved +120 V and −120 V bias lines. The response with zero bias is also shown for completeness. Near the center frequency, the emitted sound is reduced by about 25 dB (Figure 2). Power spectra of these signals are given in Figure 3.

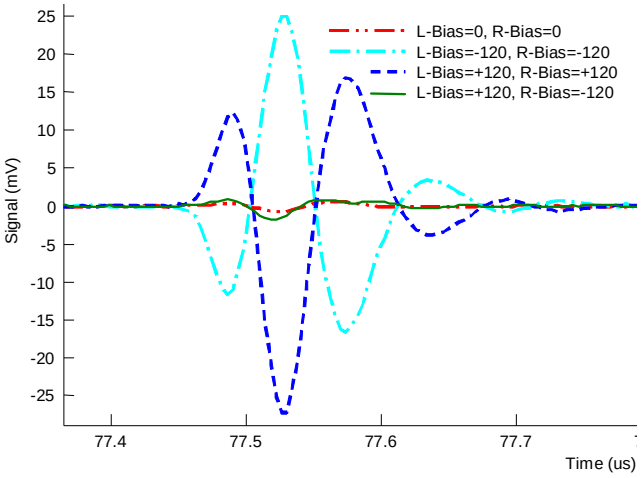

Figure 2: Suppression of sound output with alternating bias pattern. The dark blue signal is for +120 V bias, light blue is -120 V, red is spatially alternating ±120 V with 208 μm period, and the green is with 0 V bias.

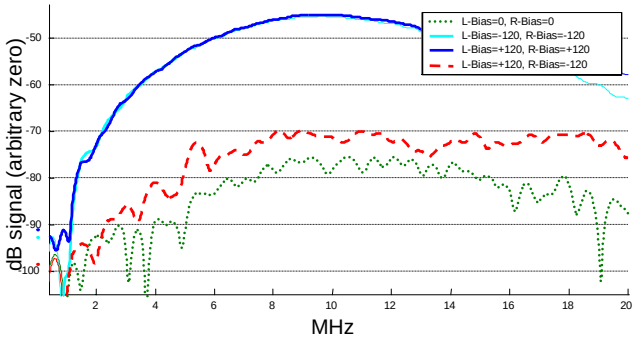

Figure 3: Power spectra of previous signals showing attenuation with alternating bias over a wide frequency range. "L-Bias" and "R-Bias" refer to odd- and even-numbered bias lines, respectively.

Next, a bias pattern was set up to focus at 20 mm. A simple way to achieve this is to compute the required phase φ for a bias line at elevation *y*, geometrically:

$$\varphi = 2\pi f\,[\sqrt{(r^2 + y^2)} - r] / c$$

where *r* is the focal depth, *f* is the frequency, and *c* is the sound speed. Then the bias voltage sign *s* becomes:

$$s = \text{sign}[\text{mod}(\varphi, 2\pi) - \pi]$$

The previous equations are for single-frequency operation, so we developed an optimizer to find the best bias line patterns for broadband operation. We used a 2-cycle burst (60% half-power fractional bandwidth). Simulations and experimental results at 20 mm are shown in Figure 4.

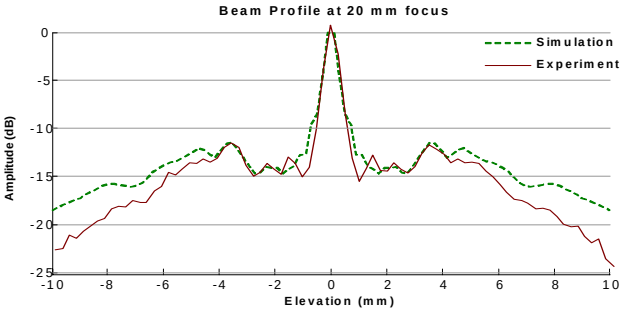

Figure 4: Comparing simulation and experiment for a Fresnel focus at 20 mm. Simulation (green) and experiment (brown) match well.

Figure 5 shows measured broadband bias line focusing at 40 mm.

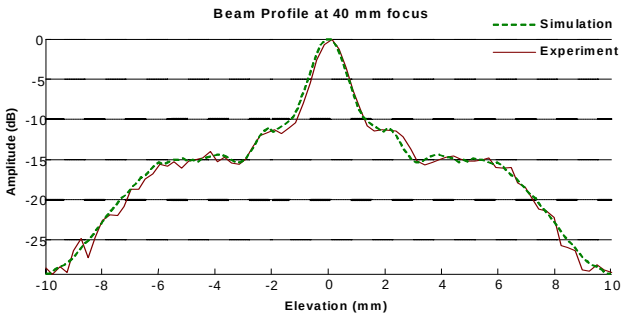

Figure 5: A 40 mm elevation focus, also with good simulation-experiment agreement.

IV. IMPROVED BEAM PROFILES

The optimizer can be given various goals, weighing sensitivity, main lobe width, and side lobe levels. Figure 6 shows beam profiles it produced with two different criteria of "goodness".

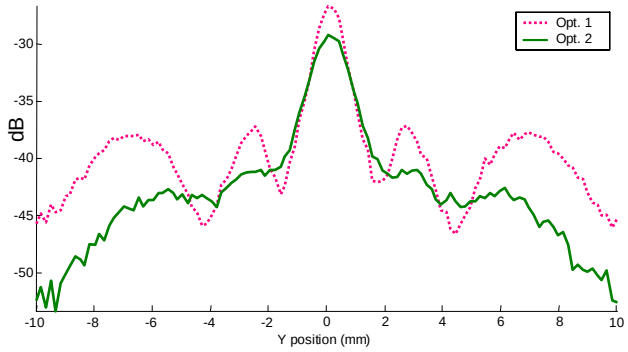

Figure 6: Experimental data for 60 mm focus, using optimized bias line patterns to create beam profiles with different characteristics.

Another way to improve the beam profile is to fire twice, and then add these firings with a phase shift of 90° at the center frequency. In radiology, tissue motion is usually slow enough that 2-3 firings can be added without loss of coherence. This improves performance quite markedly, as can be seen in Figure 7 and Figure 8. Introducing this 90° phase shift makes it possible to break the symmetry of the aperture, and offers the possibility of some steering of the beam.

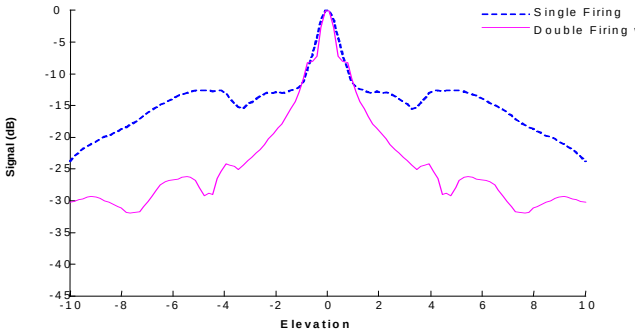

Figure 7: Simulation of the effect of combining two firings with different bias patterns. The second firing is 90° phase-shifted from the first.

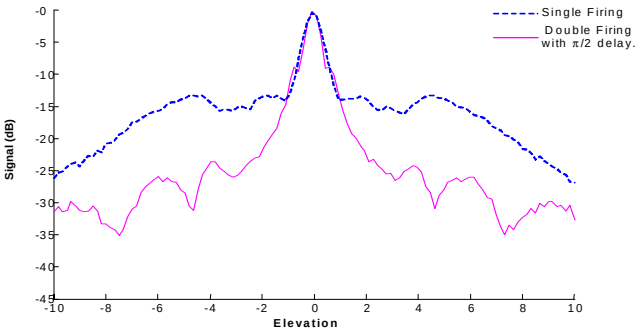

Figure 8: Experimental confirmation of two-firing scheme with 90° phase shift.

An attractive feature of this approach to reducing slice thickness is that to the system, the probe largely appears to be a 1-D device. The system software merely informs the probe of the current focal zone number. No increase in cable count is needed, and the pitch of the interconnect within the probe is the same as for 1-D. The cost can thereby be kept low.

V. HARMONIC IMAGING

When the bias applied to a cMUT is not much greater than its RF excitation, the output pressure is non-linearly related to the RF voltage. This nonlinearity only exists in transmission. There are two sources of nonlinearity: for a constant gap, the pressure is proportional to the square of the applied RF voltage. Also, for a constant voltage, the pressure is roughly dependent on d^{-2}, where d is the gap. The derivation is beyond the scope of this paper, but it can be shown

that when these effects are combined, the phase of the transmitted pressure has the same sign as that of each source of nonlinearity operating separately. These phase relationships are summarized in Table 1.

Table 1: Signs of fundamental, f_o, and harmonic signals transmitted for bias voltages with the same, and opposite signs than the RF drive voltage.

Signs of Bias and AC signal	Same	Opposite
f_o	H_1	$-H_1$
$2{\cdot}f_o$	H_2	H_2
$3{\cdot}f_o$	H_3	$-H_3$
$4{\cdot}f_o$	H_4	H_4

A very useful consequence of this is that the alternating bias pattern at maximum spatial frequency (described in section III) produces *only even harmonics* when the cMUT is driven into significant nonlinearity. We can use this to cancel harmonics at any drive level with the simple three-firing scheme detailed in Table 2. Consider transmitting the two signals used in standard pulse inversion harmonics $p(+V_{AC})$ and $p(-V_{AC})$ and coherently summing the received signal. Then transmit $p(AltBias)$, a signal with the alternating bias pattern of section III, and subtract twice the received signal:

$$\text{Image} = p(+V_{AC}) + p(-V_{AC}) - 2{\cdot}p(AltBias)$$

Table 2: A three-firing scheme which produces a harmonic image with no transmitted second harmonic contamination, without pre-distorting the RF drive.

Signal	$+V_{DC}+V_{AC}$	$+V_{DC}-V_{AC}$	$-2{\cdot}AltBias$
f_o	H_1	$-H_1$	0
$2{\cdot}f_o$	H_2	H_2	$-2{\cdot}H_2$
$3{\cdot}f_o$	H_3	$-H_3$	0
$4{\cdot}f_o$	H_4	$-H_4$	$-2{\cdot}H_4$
$2{\cdot}f_o$ (tissue)	tissue harmonic	tissue harmonic	0

The result of this pulse sequence is complete cancellation, in time and space, of the harmonics generated by the cMUT. This is independent of the amplitudes and phases of the harmonic signals, and their propagation and diffraction. It works with any transmit signal—in particular, no pre-distortion of the transmit voltage is unnecessary.

VI. Conclusions

Elevation bias line control creates a Fresnel lens in a cMUT and offers a simple way to improve slice thickness. This increases the diagnostic value of the image, and offers several additional advantages: first, such a transducer does not need a silicone lens. Even carefully designed lenses significantly worsen image SNR. Further penetration improvements accrue from the larger elevation aperture (our test array was about 3x larger in elevation than a standard transducer.) These benefits do not require significant system modifications or finer interconnect pitch.

The side lobe level is improved substantially by adding a second firing with a 90° phase shift. In this mode, performance exceeds that of commercially available multi-row transducers. Lastly, a three firing sequence with the Fresnel transducer enables harmonic imaging without pre-distortion of the transmit signal.

VII. References

[1] M. Haller and B.T. Khuri-Yakub, "A surface micromachined electrostatic ultrasonic air transducer," *1994 IEEE Ultrasonics Symposium Proceedings*, 1241-1244.

[2] C.M.W. Daft, D.G. Wildes, L.J. Thomas, L.S. Smith, R.S. Lewandowski, W.M. Leue , K.W. Rigby, C.L. Chalek and W.T. Hatfield. "A 1.5D transducer for medical ultrasound," *1994 IEEE Ultrasonics Symposium Proceedings*, 1491-1496.

[3] D.G. Wildes, R.Y. Chiao, C.M.W. Daft, K.W. Rigby, L.S. Smith, and K.E. Thomenius, "Elevation Performance of 1.25D and 1.5D Transducer Arrays," *IEEE Trans. UFFC* **44**(5), 1027-1037, 1997.

[4] I. Ladabaum, X.C. Jin, H.T. Soh, A. Atalar, and B.T. Khuri-Yakub, "Surface micromachined capacitive ultrasonic transducers," *IEEE Trans. UFFC* **45**(3), 678-690, 1998.

[5] H.D. Hristov, "Fresnel Zones in wireless links, zone plate lenses and antennas," Boston: Artech House 2000.